

10-22-2009

# Probes of Nearly Conformal Behavior in Lattice Simulations of Minimal Walking Technicolor

Simon Catterall  
*Syracuse University*

Joel Giedt  
*Rensselaer Polytechnic Institute*

Francesco Sannino  
*CP3-Origins*

Joe Schneible  
*Syracuse University*

Follow this and additional works at: <http://surface.syr.edu/phy>

 Part of the [Physics Commons](#)

## Repository Citation

Catterall, Simon; Giedt, Joel; Sannino, Francesco; and Schneible, Joe, "Probes of Nearly Conformal Behavior in Lattice Simulations of Minimal Walking Technicolor" (2009). *Physics*. Paper 439.  
<http://surface.syr.edu/phy/439>

This Article is brought to you for free and open access by the College of Arts and Sciences at SURFACE. It has been accepted for inclusion in Physics by an authorized administrator of SURFACE. For more information, please contact [surface@syr.edu](mailto:surface@syr.edu).

# Probes of nearly conformal behavior in lattice simulations of minimal walking technicolor

♣ Simon CATTERALL,<sup>\*</sup> ♠ Joel GIEDT,<sup>†</sup> ♥ Francesco SANNINO,<sup>‡</sup> and ♣ Joe SCHNEIBLE<sup>§</sup>

♣ *Department of Physics, Syracuse University, NY 13244.*

♠ *Department of Physics, Applied Physics and Astronomy,  
110 8th St., Rensselaer Polytechnic Institute, Troy, NY 12180 USA.*

♥ *CP<sup>3</sup>-Origins, Campusvej 55, DK-5230 Odense M, Denmark.*¶

(Dated: Oct. 22, 2009)

## Abstract

We present results from high precision, large volume simulations of the lattice gauge theory corresponding to minimal walking technicolor. We find evidence that the pion decay constant vanishes in the infinite volume limit and that the dependence of the chiral condensate on quark mass  $m_q$  is inconsistent with spontaneous symmetry breaking. These findings are consistent with the all-orders beta function prediction as well as the Schrödinger functional studies that indicate the existence of a nontrivial infrared fixed point.

PACS numbers: 11.15.Ex, 11.15.Ha, 12.60.Nz

---

¶ Centre of Excellence for Particle Physics Phenomenology devoted to the understanding of the Origins of Mass in the universe.

\*Electronic address: smc@physics.syr.edu

†Electronic address: giedtj@rpi.edu

‡Electronic address: sannino@cp3.sdu.dk

§Electronic address: jschneib@physics.syr.edu

## I. MINIMAL CONFORMAL GAUGE THEORIES

Depending on the number of flavors, matter representation and colors, non-abelian gauge theories are expected to exist in a number of distinct phases, classifiable according to the force felt between two static sources. The knowledge of this phase diagram is relevant for the construction of extensions of the Standard Model (SM) that invoke dynamical electroweak symmetry breaking [1, 2]. It is also useful in providing ultraviolet completions of unparticle models [3, 4, 5].

“Minimal walking technicolor” and similar models employ fermions in higher dimensional representations of the new gauge group [6, 7, 8, 9, 10]. It is thought that some of these theories will develop a non-trivial infrared fixed point (IRFP) for a small number of flavors [6, 11]. The presence of a *bona fide* IRFP requires the vanishing of the beta function for a certain value of the coupling. However, it may be possible (at least in perturbation theory) to find a scheme where the beta function has a zero yet no IRFP actually exists; indeed there are known examples in supersymmetric theories, when the beta function is written in ’t Hooft’s scheme [12]. On the other hand, if the beta function is written in a scheme that uniquely and correctly determines scheme-independent quantities at the fixed point — such as the anomalous dimension (scaling exponent) of the fermion mass operator — then it is a “physical” beta function. We discuss such a beta function in this article — the conjectured all-orders beta function (cf. Eq. (2.2) below). It vanishes at  $g = g_*$  such that  $\beta_0 - \frac{2}{3}T(r)N_f\gamma(g_*^2) = 0$  where  $\gamma(g^2)$  is the anomalous dimension of  $\bar{\psi}\psi$  and  $T(r)$  is the Dynkin index of the representation  $r$  and  $N_f$  is the number of flavors. Since the one-loop coefficient  $\beta_0$  is universal, it can be seen that in this scheme the vanishing of the beta function leads to an unambiguous result for  $\gamma(g_*^2)$ , which is physical.

Historically a nearly conformal behavior has been identified with the slow rise of the coupling constant, in an unspecified renormalization scheme, as the energy scale is reduced. Such a slow rise was termed *walking* behavior [13, 14, 15, 16]. It can be shown that this is a scheme dependent statement (a nice illustration was made in [17]). We expect, however, that a large anomalous dimension in an on-shell scheme is meaningful in the desired fashion — it generates a condensate that is large compared to the scale “ $\Lambda_{QCD}$ ” of the theory.

In order to better establish the location of the conformal window in minimal walking technicolor models there have recently been a number of lattice studies<sup>1</sup>[18, 19, 20, 21, 22, 23, 24, 25, 26]. These investigations indicate that these gauge

---

<sup>1</sup> Searches for the conformal window in theories with fundamental representation quarks have also

theories are nearly or actually conformal, as predicted in [6, 11]. Conformality at large distances implies scale invariance, which forbids a chiral condensate. Stable lattice simulations require a small but nonzero fermion mass, which ensures that the lattice theory will possess a condensate. The condensate vanishes when the mass is extrapolated to zero at finite volume, so lattice measurements of the condensate must be analyzed carefully to disentangle the infinite volume, zero mass continuum behavior from the effects of small but non-zero quark masses and finite volumes. In principle, we should be able to distinguish true scale invariance from walking behavior via a careful study of the spectrum and chiral condensate. The point is that the two cases will show different behavior as the mass and inverse volume are sent to zero, where the latter extrapolation should be performed first. This will be the aim of the current study which focuses on the minimal walking technicolor model. This is an  $SU(2)$  gauge theory with two Dirac flavors (four Weyl or Majorana fermions<sup>2</sup>) transforming according to the adjoint representation of the gauge group. The global quantum symmetry group is  $SU(4)$ . A Majorana mass term reduces this to  $SO(4)$ . The lattice results that we report here are a continuation of our earlier work [18, 19]. We will present results with spatial volumes of  $8^3, 12^3, 16^3$  and  $24^3$ , at several values of the quark mass. We are able to see trends in the finite size effects that are quite intriguing.

In Section II we start with a brief summary of the analytical predictions, making use of the old and new approaches. In addition we discuss the effect of introducing a non-zero fermion mass in a gauge theory that is otherwise conformal. Section III reviews our lattice simulation results. This is followed by an interpretation in Section IV. Some experiments with clover fermions are summarized in Section V, and we find that this improvement should allow us to explore the  $\epsilon$  and  $\delta$  regimes in a future work. We conclude with a discussion in Section VI.

## II. THEORETICAL CONSIDERATIONS

We discuss here  $SU(N)$  gauge theory with  $N_f$  Dirac fermions in the adjoint representation, and the critical number of flavors  $N_f^{cr}$  below which scale invariance is broken. Because the quarks and gluons are in the same representation, it is reasonable to assume that  $N_f^{cr}$  is independent of the number of colors  $N_c$  (this is certainly

---

received recent attention [27, 28, 29, 30, 31]

<sup>2</sup> Since we add a mass term in the lattice formulation, it is the Majorana description which is more appropriate.

true in perturbation theory).

### A. Truncated Schwinger-Dyson

The first analysis of the phase diagram with fermions in higher dimensional representations used truncated Schwinger-Dyson (SD) equations, with fermions in the two-index symmetric or antisymmetric representation [6]. For  $N_c = 2$ , the two-index symmetric representation is the adjoint representation. The generalization of the SD approach to any representation was carried out in [8], yielding for the adjoint the conformal window

$$2.075 \lesssim N_f^{\text{SD}} < \frac{11}{4} = 2.75. \quad (2.1)$$

In terms of Weyl fermions the window becomes  $4.15 \lesssim N_{Wf}^{\text{SD}} \leq 5.5$  where the upper limit is the number of flavors above which asymptotic freedom is lost. The lower limit corresponds to the point when the SD equation can no longer be trusted and the anomalous dimension of the mass term is close to unity. Thus a theory of five Weyl fermions in the adjoint representation would appear to be in the conformal window, but one is uncertain what really occurs for the case of four Weyl fermions — equivalent to  $N_f = 2$  Dirac fermions. Our lattice study seeks to address this question; however, we first describe another analytical estimate. We mention in passing that the approach developed in [32] provides no useful constraint for any theory with fermions in higher dimensional representations as shown in [33, 34].

### B. All-orders beta function and anomalous dimension

Specializing the recently conjectured “all-orders beta function” [11] to fermions in the adjoint representation, the  $\beta$ -function reads:

$$\beta(g) = -\frac{g^3}{(4\pi)^2} \frac{\beta_0 - \frac{2}{3}N_c N_f \gamma(g^2)}{1 - \frac{g^2}{8\pi^2} N_c \left(1 + \frac{2\beta'_0}{\beta_0}\right)}, \quad (2.2)$$

where  $\beta'_0 = N_c(1 - N_f)$  and  $\beta_0 = \frac{N_c}{3}(11 - 4N_f)$  is the one-loop coefficient.

The all-orders beta function satisfies a number of consistency checks. (i) The (exact) super-Yang-Mills result is recovered for  $N_f = 1/2$ . (ii) It compares well with the running of the Yang-Mills coupling constant as determined by lattice gauge theory. (iii) It provides predictions consistent with the SD approach for a critical value of  $\gamma^c = 1$ . (iv) The conformal window matches the one obtained by a conjectured dual gauge theory.

Item (iv) relates to recent exact solutions of the 't Hooft anomaly matching conditions [35, 36]. Further developments appeared in [37]. Naturally (2.2) reduces to the well-known two-loop beta function one when expanding to  $\mathcal{O}(g^5)$ . We give it here since we will compare to it in the discussion below:

$$\beta(g) = -\frac{\beta_0}{(4\pi)^2}g^3 - \frac{\beta_1}{(4\pi)^4}g^5, \quad (2.3)$$

with (scheme independent) adjoint representation coefficients

$$\beta_0 = \frac{N_c}{3}(11 - 4N_f), \quad \beta_1 = \frac{N_c^2}{3}(34 - 32N_f). \quad (2.4)$$

We will also make use of the anomalous dimension  $\gamma = -d \ln m / d \ln \mu$  of the renormalized mass  $m$  to second order

$$\gamma = \frac{6N_c g^2}{(4\pi)^2} + \frac{2N_c(53N_c - 5N_f)g^4}{3(4\pi)^4} + \mathcal{O}(g^6) \quad (2.5)$$

The all-orders beta function predicts the anomalous dimensions of the fermion mass at the infrared fixed point and is in this sense “physical.” In [11] it was argued that the size of the conformal window is determined by the largest value allowed for the anomalous dimension,  $\gamma_c$ :

$$\frac{11}{2(2 + \gamma^c)} \leq N_f^{\text{BF}} < \frac{11}{4}. \quad (2.6)$$

The fixed point value is

$$\gamma_* = \frac{11 - 4N_f}{2N_f}. \quad (2.7)$$

(It is interesting to note that if we take  $N_f = 2$ , then  $\gamma_* = 3/4$  and the lower end of the conformal window in (2.6) is exactly  $N_f = 2$ .) If we use the SD inspired condition  $\gamma^c = 1$  we would have

$$1.8\bar{3} \leq N_f^{\text{BF}} < \frac{11}{4} \quad (2.8)$$

whereas the maximal conformal window is achieved in the unitarity limit  $\gamma^c = 2$ :

$$1.375 \leq N_f^{\text{BF}} < \frac{11}{4}. \quad (2.9)$$

What is important to notice is that independently of which of these  $\gamma^c$  is chosen, the prediction [5, 11] is that the adjoint theory with  $N_f = 2$  has an IRFP and an associated anomalous dimension  $\gamma = 3/4$ . Our aim here is to scrutinize this prediction of the all-orders beta function using lattice techniques.

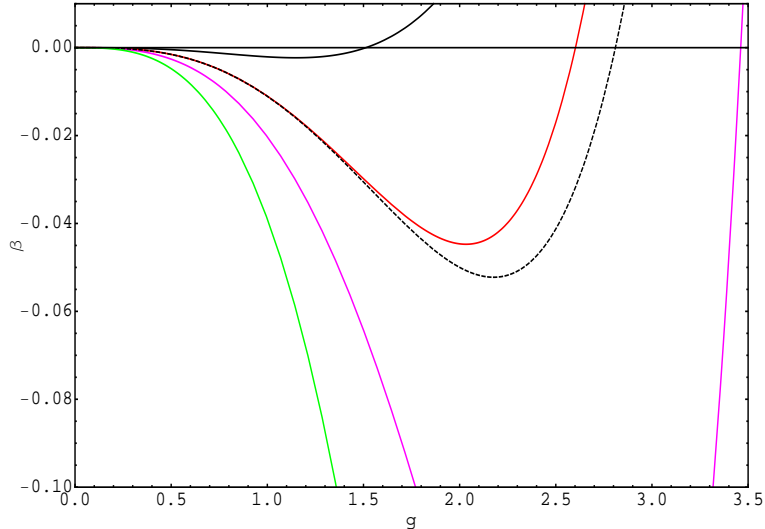


FIG. 1: Beta functions for different values of the number of Dirac flavors in the adjoint representation of the  $SU(2)$  gauge group. The black solid curve corresponds to  $N_f = 2.5$ , the red to  $N_f = 2$ , the dashed one is the two-loop beta function for  $N_f = 2$  again, while the magenta curve corresponds to  $N_f = 1.5$ . The green curve is the beta function for super Yang-Mills.

### C. Large anomalous dimensions at weak coupling

Often, in the literature, one finds plotted a cartoon of the running of the coupling constant for either conformal or nearly conformal theories. Here we provide yet another cartoon of this running but this time using the “physical” form of the conjectured all-orders beta function [11]. In order to be explicit, we augment this with a simplifying ansatz for the dependence of the anomalous dimension on the coupling constant, Eq. (2.5). The advantage is that we will be able to plot what happens when changing the number of flavors — but this is only a “cartoon” since we do not actually know what  $\gamma(g^2)$  really is in the true theory. Thus, suppose we use the two-loop expression of the anomalous dimension together with the all-orders beta function. Then the beta function for various values of  $N_f$  are shown in Fig. 1. We have also plotted the two-loop beta function for  $SU(2)$  with  $N_f = 2$ . Interestingly the fixed point is reached before the one from the two-loop beta function. (This is consistent with the recent lattice results obtained in [25].)

What one should note from Fig. 1 is that a relatively small value of  $g_*^2/(16\pi^2)$  is obtained while  $\gamma_* = \mathcal{O}(1)$ . Visually, this is because there is a long renormalization

group trajectory that must be traversed in going from a  $g \approx 0$  weak coupling value to the  $g_*$  fixed point. The curve deepens as the number of flavors is decreased from  $N_f = 2.5, 2, 1.5$ , consistent with the ordering of the fixed point values  $\gamma_* = 1/5, 3/4, 5/3$ . The general message is that one can have large values of the anomalous dimensions and yet have coupling constants at the IRFP which are small.

#### D. The chiral condensate

We have measured the chiral condensate through the GMOR relation:

$$(m_\pi f_\pi)^2 = -2m_q \Sigma. \quad (2.10)$$

Here  $\Sigma = \langle \bar{\psi}\psi \rangle$  is the condensate in infinite volume. The GMOR relation just follows from chiral symmetry breaking with a small source  $m_q$  for the “scalar current”  $\bar{\psi}\psi$ . In the case of an IRFP  $\Sigma$  must also vanish as  $m_q \rightarrow 0$ . Different scenarios for how it vanishes have been discussed in [38]. The generic expectation is that in theories where the anomalous dimension  $\gamma < 1$  or theories where instanton effects are important such as the model analyzed here,  $\Sigma \sim m_q \Lambda_U^2$  with  $\Lambda_U$  a high energy scale characterizing the onset of asymptotic freedom. In contrast QCD-like theories with chiral symmetry breaking possess a non-vanishing condensate as  $m_q \rightarrow 0$  in infinite volumes.

#### E. Finite volume effects

Lattice simulations are necessarily performed on a finite four-dimensional volume, which we will denote  $L^3 \times T$ , associating  $T$  with the extent of the temporal dimension. If the theory possesses an IRFP, then in the chiral limit  $m_q \rightarrow 0$ , large finite-size effects will always be present.

It is well-established that there are three regimes possible for lattice gauge theories with spontaneous chiral symmetry breaking; the p-regime where  $m_\pi L \gg 1$  and  $m_\pi T \gg 1$ , the  $\epsilon$ -regime where  $m_\pi L \ll 1$  and  $m_\pi T \ll 1$  and the  $\delta$ -regime with  $m_\pi L \ll 1$  but  $m_\pi T \gg 1$ . In the small volume  $\delta$  or  $\epsilon$  regime the chiral condensate will typically scale to zero linearly with quark mass in a manner similar to that expected in a theory with a IRFP. Thus we must be particularly careful in interpreting our lattice results on small boxes in order to distinguish the two scenarios.

Indeed, it is not clear that this categorization will prove useful in a theory that has an IRFP, where there is no spontaneous chiral symmetry breaking. The difficulty is that the expansion parameters and mode decoupling arguments rely heavily on

$f_\pi \neq 0$  in the chiral, infinite volume limit. This is not true for the theory with an IRFP.

### III. LATTICE ANALYSIS

For details of our lattice action and simulation algorithm we refer the reader to [19]. Suffice it to say that we have employed unimproved Wilson fermions in the adjoint representation and a simple Wilson plaquette action for the gauge field and generated configurations using the usual HMC algorithm. We now turn to the extraction of accurate estimates of the meson and quark masses and the pion decay constant  $f_\pi$ .

#### A. Current quark mass extraction

The fermion mass  $m_q$  is obtained from a fit to

$$G_{PCAC}(t) = \frac{\partial_t G_{AP}(t)}{G_{PP}(t)} \approx \frac{2Z_m Z_P m_q}{Z_A} \equiv 2m_{PCAC}, \quad 0 \ll t \ll T. \quad (3.1)$$

Here,  $T$  is the number of sites in the temporal direction,  $m_{PCAC}$  is the bare PCAC mass and  $m_q$  is the renormalized current quark mass. In this work we do not determine the renormalization constants  $Z_m, Z_P, Z_A$ ; however they are expected to be  $\mathcal{O}(1)$  and we will suppress them in much of what follows. The two Green's functions involved in (3.1) are:

$$G_{PP}^{ab}(t) = \int d^3x \langle P^a(t, \mathbf{x}) P^b(0, \mathbf{0}) \rangle, \quad G_{AP}^{ab}(t) = \int d^3x \langle A_0^a(t, \mathbf{x}) P^b(0, \mathbf{0}) \rangle, \quad (3.2)$$

where  $P^a = \bar{\psi} \gamma_5 t^a \psi$  and  $A_0^a = \bar{\psi} \gamma_0 \gamma_5 t^a \psi$ , with  $t^a \in \{\sigma^+, \sigma^-, \sigma^3\}$ . For brevity we suppress the isospin indices  $a, b$  and leave it as implied that the nonvanishing components  $G^{+-}$  (i.e. the ones without disconnected diagrams) of the Green's functions are used in the measurements. At leading order in the expansion of states,

$$G_{PP}(t) \sim \partial_t G_{AP}(t) \sim \cosh \left[ m_\pi \left( \frac{T}{2} - t \right) \right], \quad 0 \ll t \ll T. \quad (3.3)$$

This is why a constant is expected in (3.1). The integral over  $\mathbf{x}$  in Eq. (3.2) projects onto zero momentum states. In practice we approximate  $\partial_t \approx \nabla_t^{(S)}$ , the symmetric difference operator.

## B. Meson masses and decay constants

Next we describe how  $m_\pi$  and  $f_\pi$  are measured. Referring to the correlation function  $G_{PP}(t)$ , we work in the leading exponential approximation:

$$G_{PP}(t) = C_{PP} \cosh \left( m_\pi \left( \frac{T}{2} - t \right) \right) \quad (3.4)$$

On the other hand, using the resolution of the identity in terms of states,

$$G_{PP}(t) = \frac{1}{2m_\pi} |\langle 0|P(0, \mathbf{0})|\pi, \mathbf{q} = 0 \rangle|^2 2e^{-m_\pi T/2} \cosh \left( m_\pi \left( \frac{T}{2} - t \right) \right) \quad (3.5)$$

neglecting excited state contributions. The matrix element  $\langle 0|P(0, \mathbf{0})|\pi, \mathbf{q} = 0 \rangle$  is well known:

$$\langle 0|P(0, \mathbf{0})|\pi, \mathbf{q} = 0 \rangle = \frac{m_\pi^2 f_\pi}{2Z_m Z_p m_q} \quad (3.6)$$

Thus we obtain:

$$f_\pi = \left( \frac{C_{PP}}{m_\pi^3} \right)^{1/2} 2Z_m Z_p m_q e^{m_\pi T/4} \quad (3.7)$$

This is then combined with (3.1) to obtain  $f_\pi^{\text{bare}} \equiv f_\pi/Z_A$ .

## C. Results at $\beta = 2.05$

First we discuss results from simulations at  $\beta = 2.05$  on a  $L^3 \times 32$  lattice with periodic boundary conditions imposed in all directions. For  $L = 8, 12, 16$  a total of 10500 HMC trajectories were generated. For  $L = 24$ , a total of approximately 5000 HMC trajectories were generated. In all cases, the first 200 were discarded as thermalization and observables were obtained by averaging from every tenth trajectory of the remaining ensemble. Errors were corrected for autocorrelations in the data. We performed nonlinear fits to (3.3). We estimated the statistical uncertainty by the jackknife method, fitting repeatedly with a block of data removed. Jackknife block sizes of 10, 25, 50, 100 and 200 all gave consistent results, including error estimates.

The fit results depend significantly on the range of  $t$  that is included, due to excited state contamination. The variable  $t_{\text{first}}$  determines the first timeslice that is included. An example of the fit variation is given in Fig. 2. It can be seen that there is a plateau that is reached as  $t_{\text{first}}$  is increased. In practice we fit to a constant plus exponential

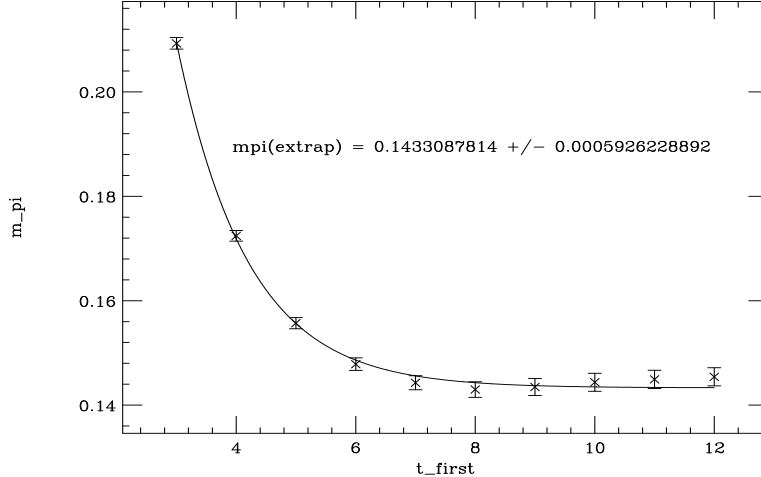


FIG. 2: Estimates of  $m_\pi a$  for  $\beta = 2.05$ ,  $8^3 \times 32$  lattice as the beginning of the fit range,  $t_{\text{first}}$ , is varied.

$L$	$ma$	$m_\pi a$	$m_\rho a$	$f_\pi a$	$m_q a$	$Ra^2$
8	-1.29	0.5686(9)	0.6010(6)	0.619(7)	0.1078(5)	11.08(10)
8	-1.30	0.3680(10)	0.3952(12)	0.668(10)	0.0685(3)	13.40(15)
8	-1.31	0.1433(6)	0.1530(9)	0.738(9)	0.0253(2)	19.55(8)

TABLE I:  $\beta = 2.05$ ,  $L^3 \times 32$  PBC lattice, with unimproved Wilson quarks.

decay with  $t_{\text{first}}$ , and use the constant with fitting error as our estimate of a given observable.

Results are shown in Tables I (mass variation) and II (volume variation). The quantity  $R$  will be discussed in a subsequent section. It can be seen that  $f_\pi$  decreases significantly with volume, whereas the behavior of the pion and rho masses are more complicated. Further numerical analysis is presented in Table III, which shows that a significant splitting of the rho and pion occurs for large enough volume and small enough quark mass. This table also shows that we are far from the heavy quark limit where  $m_\pi \approx 2m_q$  would hold.

#### D. Results at $\beta = 2.5$

Next we discuss results for  $\beta = 2.5$ . Here we have also allowed for a larger time extent,  $T = 64$ , in order to account for what might be a finer lattice spacing. The

$L$	$ma$	$m_q a$	$m_\pi a$	$m_\rho a$	$f_\pi a$	$Ra^2$
8	-1.31	0.0253(2)	0.1433(6)	0.1530(9)	0.738(9)	19.55(8)
12	-1.31	0.015236(63)	0.1215(17)	0.1547(24)	0.4598(29)	13.83(14)
16	-1.31	0.01214(16)	0.1075(15)	0.1531(25)	0.406(10)	13.854(76)
24	-1.31	0.00800(11)	0.1254(42)	0.1770(59)	0.1743(46)	8.25(25)

TABLE II: Quantities of interest for the  $\beta = 2.05$ ,  $L^3 \times 32$  PBC lattice, with unimproved Wilson fermions.

$L$	$m_q a$	$m_\pi/m_q$	$(m_\rho - m_\pi)/m_\pi$
8	0.0253(2)	5.664(51)	0.0677(77)
12	0.015236(63)	7.97(12)	0.273(27)
16	0.01214(16)	8.86(17)	0.424(31)
24	0.00800(11)	15.68(57)	0.411(67)

TABLE III: Pion mass and rho-pion splitting enhancement as  $m_q$  and  $1/L$  are decreased, for the  $\beta = 2.05$ ,  $L^3 \times 32$  PBC lattice, with unimproved Wilson fermions.

fits versus  $t_{\text{first}}$  are similar to Fig. 2. The method of simulation, sampling and fits are the same as for  $\beta = 2.05$ . Results are given in Table IV.

#### IV. INTERPRETATION

In this section we characterize the numerical results. First consider the quantity  $R \equiv (m_\pi f_\pi/m_q)^2 = \Sigma/m_q$ . By our earlier arguments, for a theory with an IRFP, this should approach a constant in the chiral limit  $m_q \rightarrow 0$ . In a QCD-like theory,

$L$	$ma$	$m_\pi a$	$m_\rho a$	$f_\pi a$	$m_q a$	$Ra^2$
8	-1.1	0.13625(7)	0.14531(5)	1.039(12)	0.03834(3)	13.621(15)
12	-1.1	0.12260(7)	0.13537(15)	0.593(11)	0.02900(11)	6.091(6)
16	-1.1	0.1204(2)	0.1251(7)	0.405(5)	0.0284(4)	2.957(13)
24	-1.1	0.1344(12)	0.1497(6)	0.242(2)	0.0266(3)	1.49(3)

TABLE IV: Quantities of interest for the  $\beta = 2.5$ ,  $L^3 \times 64$  PBC lattice, with unimproved Wilson fermions.

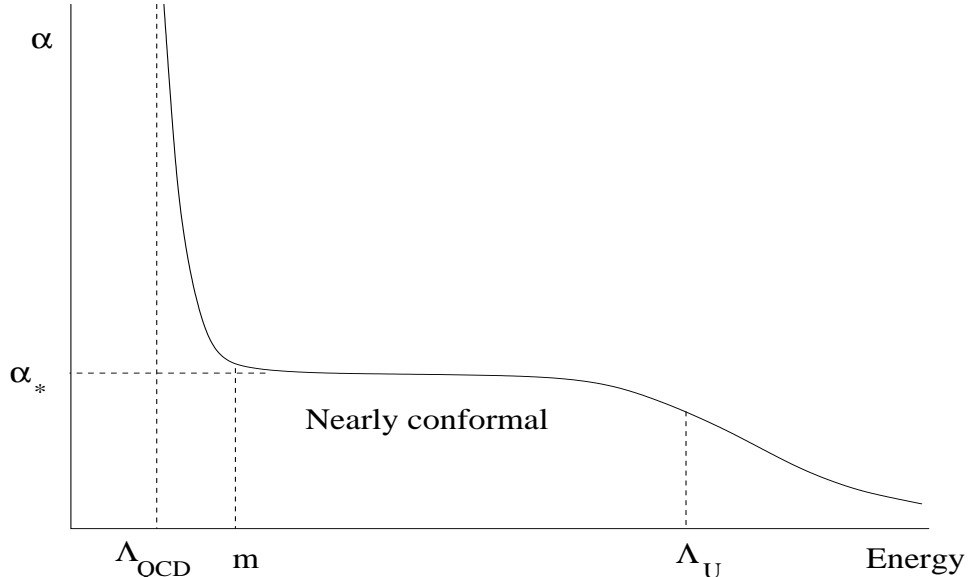


FIG. 3: Nearly conformal flow for a theory that would have an IRFP when  $m = 0$ . The dynamical scale “ $\Lambda_{QCD}$ ” is generated below the mass scale  $m$ .

the order of limits (chiral versus thermodynamic) matters. If  $L \rightarrow \infty$  before taking the chiral limit, then  $R$  would diverge inversely with the quark mass  $m_q$ . In the  $\delta$ - or  $\epsilon$ -regime one has instead  $\Sigma \sim m_q$ , which would lead to a finite result for  $R$  in the chiral limit. Our values of  $m_\pi L$  at the pseudo-critical values of bare mass  $ma$  range from 1.1 to 3.0, whereas in the  $\delta$ - or  $\epsilon$ -regime one has  $m_\pi L \ll 1$ . Thus on our larger lattices we are certainly outside of these small volume regimes. In Tables II and IV we observe  $R$  decreasing as  $L$  increases. This stands in stark contrast to what would happen in a QCD-like theory that is outside of the small volume regimes. For this reason we find that our data favors the IRFP interpretation, as far as the chiral condensate is concerned. In fact, we find that  $R \sim 1/L^2$ , as a result of the observed scaling  $f_\pi \sim 1/L$ . This seems to be evidence for a vanishing condensate at large  $L$ , consistent with the existence of an IRFP. However, we cannot rule out a small but nonvanishing infinite volume condensate; i.e., it is possible that we could just be seeing a decreasing finite volume effect that is much larger than the infinite volume piece for the lattices we are studying.

The vanishing of the decay constant  $f_\pi$  with increasing lattice volume contrasts starkly with the approximate volume independence of the pion (and rho) masses shown in Tables II and IV. The origin of this behavior is difficult to understand. However, we can assume that at distances scales longer than the inverse quark mass

the fermions effectively decouple from the dynamics leaving an IR theory which behaves like quenched QCD but with a light scale

$$\Lambda_{QCD} \sim m_q e^{-8\pi^2/g_*^2} \quad (4.1)$$

(see Figure. 3). These light gluonic states have been seen in simulations [26] at energies below that of the corresponding pion and rho states. Notice also that while the pion and rho masses do not scale with the lattice volume they are not simply the sum of the two constituent quark masses  $m_q$ , as emphasized in Table III. Instead it is best to think of the pion as being composed of two “dressed” quarks where the dressing represents the effects of these light gluonic degrees of freedom. A useful analogy would be the  $\phi$ -system in QCD composed of two strange quarks.

We can parameterize the dependence of the pion mass on the quark masses in a phenomenological way as

$$m_\pi = cm_q^{1-\tilde{\delta}} L^{-\tilde{\delta}} + \mathcal{O}(a\Lambda_{UV}^2). \quad (4.2)$$

However, this formula only explains the increase in meson masses in going from  $L = 16$  to  $L = 24$  provided the  $\mathcal{O}(a\Lambda_{UV}^2)$  effects become larger in this limit, presumably due to larger renormalizations as the number of degrees of freedom is increased. Also, in the presence of an IRFP there will be large cutoff effects because one is explicitly breaking conformality, an essential symmetry of the theory we are trying to study. The pion is no longer a pseudo-Nambu-Goldstone boson, due to the absence of spontaneous chiral symmetry breaking, hence its mass is quite sensitive to this explicit breaking of scale invariance. For this reason one expects large  $\mathcal{O}(a\Lambda_{UV}^2)$  effects, which is precisely what we observe. To be consistent with our numerical results the (positive) exponent  $\tilde{\delta}$  that appears in (4.2) should be small.

Compatibility with the GMOR relation then implies that

$$f_\pi = c' m_q^{\tilde{\delta}} L^{\tilde{\delta}-1} + \mathcal{O}(a\Lambda_{UV}^2) \quad (4.3)$$

which has the merit of guaranteeing that  $f_\pi$  vanishes both with the lattice volume and also as  $m_q \rightarrow 0$ . Because  $f_\pi$  is taken from a ratio of the lattice derivative of a correlation function to another correlation function, it is possible that large  $\mathcal{O}(a\Lambda_{UV}^2)$  cutoff effects may be absent, due to cancellations. In fact, this would explain our lattice data in the tables above, where  $f_\pi$  is seen to decrease both with  $m_q$  and  $1/L$ ; a large constant term  $\mathcal{O}(a\Lambda_{UV}^2)$  does not seem to be present. Thus it may be that the leading lattice spacing correction to  $f_\pi$  is actually  $\mathcal{O}(am_q^2)$ .

We note that our  $\beta = 2.5$  data is roughly consistent with Eqs. (4.2) and (4.3), while the  $\beta = 2.05$  is less so. For either value of  $\beta$ , the increase in the meson masses

in going from  $L = 16$  to  $L = 24$  is quite strange, and seems on its face to be at odds with variational arguments.<sup>3</sup> However, topological features could play a nontrivial role in such finite volume considerations, in a way that might resolve the apparent paradox.

## V. VALENCE CLOVER ON UNIMPROVED WILSON SEA

In order to proceed to light quark masses and move into the  $\delta$ - and  $\epsilon$ -regimes we have experimented with simulations that utilize a clover-improved Wilson-Dirac propagator. We have computed the pion mass on the same unimproved dynamical Wilson configurations described in Section III. Setting the coefficient of the clover term  $c_{SW} = \mathcal{O}(1)$ , we have been able to achieve  $m_\pi a \lesssim 0.05$  by tuning the valence quark mass. This indicates that dynamical clover fermions would allow for an exploration of the  $\delta$ - and  $\epsilon$ -regimes, something that we plan to do in a future work.

## VI. DISCUSSION

We have presented results for the low lying meson masses, decay constants and chiral condensate from simulations of the minimal walking technicolor theory corresponding to two flavors of adjoint Dirac fermions in  $SU(2)$  gauge theory. Data at two couplings  $\beta = 2.05$  and  $\beta = 2.5$  and a range of lattice volumes  $L^3 \times 32(64)$ , with  $L = 8, 12, 16, 24$  were shown. Unimproved Wilson fermions and Wilson glue are used and ensembles of  $\mathcal{O}(10000)$  configurations accumulated at each set of parameter values.

We have shown how the GMOR relation may be used to compute the chiral condensate and discussed the relationship between the condensate measured on the lattice and its continuum cousin. Our results are consistent with the vanishing of the condensate in the infinite volume limit and hence the existence of an infrared fixed point. The dependence of  $f_\pi$  and the pion and rho masses on both the quark mass and lattice volume are shown to also support the presence of such a fixed point, though other interpretations are possible.

---

<sup>3</sup> We thank R. Brower for raising this point. The essence of the argument is that on doubling the lattice size, the original pion wavefunction can be periodically extended. But one would expect that it is no longer the minimum energy eigenstate in the pseudo-scalar channel, since new basis states for a variational analysis are allowed on the larger lattice. It follows that the pion mass in the larger volume will be lower.

## Acknowledgements

JG was supported by Rensselaer faculty development funds. The work of S.C. is supported in part by DOE grant DE-FG02-85ER40237. All simulations were performed using facilities at RPI's Computational Center for Nanotechnology and Innovation.

- 
- [1] S. Weinberg, Phys. Rev. D **19**, 1277 (1979).
  - [2] L. Susskind, Phys. Rev. D **20**, 2619 (1979).
  - [3] H. Georgi, Phys. Rev. Lett. **98**, 221601 (2007)
  - [4] F. Sannino and R. Zwicky, arXiv:0810.2686 [hep-ph].
  - [5] F. Sannino, arXiv:0804.0182 [hep-ph].
  - [6] F. Sannino and K. Tuominen, Phys. Rev. D **71**, 051901 (2005)
  - [7] D. D. Dietrich, F. Sannino and K. Tuominen, Phys. Rev. D **72**, 055001 (2005)
  - [8] D. D. Dietrich and F. Sannino, Phys. Rev. D **75**, 085018 (2007)
  - [9] R. Foadi, M. T. Frandsen, T. A. Rytto and F. Sannino, Phys. Rev. D **76**, 055005 (2007)
  - [10] T. A. Rytto and F. Sannino, arXiv:0809.0713 [hep-ph].
  - [11] T. A. Rytto and F. Sannino, Phys. Rev. D **78**, 065001 (2008)
  - [12] G. 't Hooft, "The renormalization group in quantum field theory," in *Under the spell of the gauge principle*, World Scientific, Singapore, 1994.
  - [13] E. Eichten and K. D. Lane, Phys. Lett. B **90**, 125 (1980).
  - [14] B. Holdom, Phys. Rev. D **24**, 1441 (1981).
  - [15] K. Yamawaki, M. Bando and K. i. Matumoto, Phys. Rev. Lett. **56**, 1335 (1986).
  - [16] T. W. Appelquist, D. Karabali and L. C. R. Wijewardhana, Phys. Rev. Lett. **57**, 957 (1986).
  - [17] L. del Debbio, talk given at "Universe in a Box," Lorentz Center, Leiden, August, 2009.
  - [18] S. Catterall and F. Sannino, Phys. Rev. D **76** (2007) 034504.
  - [19] S. Catterall, J. Giedt, F. Sannino and J. Schneible, JHEP **0811** (2008) 009.
  - [20] Y. Shamir, B. Svetitsky and T. DeGrand, Phys. Rev. D **78**, 031502 (2008).
  - [21] T. DeGrand, Y. Shamir and B. Svetitsky, Phys. Rev. D **79**, 034501 (2009) [arXiv:0812.1427 [hep-lat]].
  - [22] L. Del Debbio, M. T. Frandsen, H. Panagopoulos and F. Sannino, JHEP **0806**, 007

- (2008).
- [23] L. Del Debbio, A. Patella and C. Pica, arXiv:0805.2058 [hep-lat].
  - [24] A. Hietanen, J. Rantaharju, K. Rummukainen and K. Tuominen, PoS **LATTICE2008**, 065 (2008).
  - [25] A. J. Hietanen, K. Rummukainen and K. Tuominen, arXiv:0904.0864 [hep-lat].
  - [26] C. Pica, L. Del Debbio, B. Lucini, A. Patella and A. Rago, arXiv:0909.3178 [hep-lat].
  - [27] T. Appelquist, G. T. Fleming and E. T. Neil, Phys. Rev. D **79**, 076010 (2009) [arXiv:0901.3766 [hep-ph]].
  - [28] T. Appelquist *et al.*, arXiv:0910.2224 [hep-ph].
  - [29] Z. Fodor, K. Holland, J. Kuti, D. Nogradi and C. Schroeder, arXiv:0907.4562 [hep-lat].
  - [30] Z. Fodor, K. Holland, J. Kuti, D. Nogradi and C. Schroeder, arXiv:0809.4890 [hep-lat].
  - [31] A. Deuzeman, M. P. Lombardo and E. Pallante, arXiv:0904.4662 [hep-ph].
  - [32] T. Appelquist, A. G. Cohen and M. Schmaltz, Phys. Rev. D **60** (1999) 045003.
  - [33] F. Sannino, Phys. Rev. D **72**, 125006 (2005).
  - [34] F. Sannino, Phys. Rev. D **79**, 096007 (2009).
  - [35] F. Sannino, Phys. Rev. D **80**, 065011 (2009).
  - [36] F. Sannino, arXiv:0909.4584 [hep-th].
  - [37] O. Antipin and K. Tuominen, arXiv:0909.4879 [hep-ph]. D. D. Dietrich, arXiv:0908.1364 [hep-th].
  - [38] F. Sannino, Phys. Rev. D **80**, 017901 (2009) [arXiv:0811.0616 [hep-ph]].